Microchemical Journal 166 (2021) 106236

Contents lists available at ScienceDirect

Microchemical Journal

journal homepage: www.elsevier.com/locate/microc

Quantitative analysis of the platinum surface decoration on lanthanum strontium iron oxide thin films via online-LASIL-ICP-MS

Maximilian Weiss [a,*], Christoph Riedl [b], Johannes Frank [c], Jürgen Fleig [b], Andreas Limbeck [a,*]

[a] TU Wien Institute of Chemical Technologies and Analytics, Getreidemarkt 9/164-I²AC, 1060 Vienna, Austria
[b] TU Wien Institute for Chemical Technologies and Analytics, Getreidemarkt 9/164-EC, 1060 Vienna, Austria
[c] TU Wien Joint Workshop Technical Chemistry, Getreidemarkt 9/164-EC, 1060 Vienna, Austria

ARTICLE INFO

Keywords:
Laser ablation of solids in liquids
ICP-MS
Imaging
Depth profiling
Mixed ionic electronic conductors

ABSTRACT

Solid oxide fuel cells (SOFCs) are one of the key technologies on the way to environmentally friendly power generation. Current research activities aim to reduce their operational temperature to intermediate temperatures (400–600 °C) to make their application more feasible. In a recent approach, lanthanum strontium iron oxide (LSF) thin film electrodes, a mixed ionic electronic conducting (MIEC) material, was decorated with tiny amounts of platinum nanoparticles, which led to a significant improvement of the oxygen reduction kinetics. To understand this material combination a precise characterization is of major interest, especially the exact amount of platinum on the surface. As the studied model-type thin film electrode requires a platinum current collector buried beneath the LSF to improve in-plane electron conductivity, a method providing quantitative information as well as sufficient depth resolution is needed.

In this work, we further improved the recently presented approach of online laser ablation of solids in liquids (LASIL), which enabled in combination with ICP-MS detection a spatially resolved analysis of the sample composition. Careful optimization of laser parameters and carrier solution led to a depth resolution of 30 nm, which allowed a clear separation of the Pt-signals from the surface decoration and the underlying current collector. The amount of platinum on the surface was determined using calibration with a matrix matched standard and validated by another method. Finally, the imaging capabilities of the proposed online-LASIL approach have been employed to assess the homogeneity of the Pt-decoration, indicating significant variations within the investigated area. Thus, further improvements in the electrochemical properties of the investigated LSF electrodes could be anticipated by fabrication of MIECs with a more homogeneous platinum decoration.

1. Introduction

Solid oxide fuel cells (SOFCs) directly convert chemical energy of fuels to electric energy at highly-efficiency and are therefore promising candidates for environmentally friendly power generation [1,2]. One of the main goals of current research activities is lowering the operation temperature of SOFCs from around 800 °C to intermediate temperatures (400 °C – 600 °C) [3,4]. This requires new electrode materials, which should offer sufficiently fast electrode kinetics even at those lower temperatures. Perovskite-type mixed ionic and electronic conductors (MIECs) are among the most promising candidates for future SOFC electrodes. In several studies, the properties of numerous MIEC materials, such as $SrTi_{1-x}Fe_xO_{3-\delta}$ [5–7], $La_xSr_{1-x}MnO_{3-\delta}$, [8] $La_{1-x}Sr_xFeO_{3-\delta}$ [9–12], $La_{1-x}Sr_xCoO_{3-\delta}$, [13–16] $La_{1-x}Sr_xFe_{1-y}Co_yO_{3-\delta}$ [17,18] $Ba_{1-x}Sr_xFe_{1-y}Co_yO_{3-\delta}$ [19,20] were investigated. Apart from faster oxygen reduction kinetics, SOFC electrode materials should exhibit morphological stability, possess high ionic and electronic conductivity, show little degradation and be compatible with other materials of the fuel cell [1].

A recent study [21] revealed lanthanum strontium iron oxide – $La_{0.6}Sr_{0.4}FeO_{3-\delta}$ (LSF64) – thin film electrodes decorated with tiny amounts of platinum show by far lower polarization resistance (e.g., faster oxygen exchange kinetics) than undecorated LSF electrodes. At lower oxygen partial pressures (0.25 mbar O_2) up to 70 times faster oxygen reduction kinetics were measured (e.g., the polarization resistance dropped from 125 Ωcm^2 to 2 Ωcm^2, at 600 °C). Moreover, platinum decorated LSF electrodes showed superior properties, such as lower degradation of the electrode and higher reproducibility of

* Corresponding authors.
E-mail addresses: maximilian.weiss@tuwien.ac.at (M. Weiss), andreas.limbeck@tuwien.ac.at (A. Limbeck).

https://doi.org/10.1016/j.microc.2021.106236
Received 2 February 2021; Received in revised form 8 March 2021; Accepted 9 March 2021
Available online 6 April 2021

resistance values.

To understand those promising systems, a precise characterization is desired, to correlate material properties, in particular the deposited amount of platinum, with electrochemical performance. This enables to further boost their performance through optimized material systems and production conditions. Besides the deposited amount of platinum per surface area, also the homogeneity of the Pt-distribution on the LSF surface is of major interest.

At first glance, this seems to be a rather simple task, done by sample digestion and liquid measurement, but for electrochemical impedance measurements of thin film electrodes (~100 nm thickness) current collector grids made out of platinum are used beneath the thin film to improve in-plane conductivity. Thus, an analytical method applicable for analyzing this special kind of samples should have enough surface sensitivity to distinguish between surface decoration and the underlying collector grids. Application of conventional digestion procedures with subsequent analysis is not feasible since a selective digestion of the surface decoration only is not possible, because the platinum originating from the current collector would mask the signal from the surface platinum decoration. Moreover, no information about the platinum distribution is accessible. To circumvent the problems associated with sample digestion, direct analysis of solid materials using solid sampling techniques is recommended [22–24]. Routinely applied direct solid-state methods such as secondary ion mass spectrometry (SIMS), glow discharge optical emission spectroscopy/mass spectroscopy (GD-OES/MS) and X-ray photoelectron spectroscopy (XPS) have their specific advantages but also drawbacks, SIMS is especially prone to matrix effects, GD-OES/MS does not enable spatially resolved measurements, and the application of XPS is limited by the comparatively poor sensitivity [25,26], which limits their applicability for this kind of material.

An alternative solid sampling technique is laser ablation inductively coupled plasma mass spectrometry (LA-ICP-MS). However, the depth resolution of the most frequently applied nanosecond laser-systems is not competitive to the techniques mentioned above, and thus does not allow a differentiation between the platinum surface decoration and the platinum current collector. The use of femtosecond lasers achieves depth resolutions of a few nanometers [27,28], but a much more costly equipment is required which is not accessible to many research groups. Moreover, for quantitative investigations the use of matrix matched reference materials is required, especially for novel classes of materials such standards are usually not available [25,29–32].

A method that fulfills the requirements stated above is laser ablation of solids in liquids (LASIL). Thereby a very fine dispersion of nanoparticulates is produced via laser ablation of a solid sample in a liquid. This method is used extensively in nanomaterial research [33,34] for the production of nanoparticles of different size and composition. The first application for analytical purposes was reported by Muravitskaya et al. [35]. In the studies reported so far [36–38] the produced nanoparticles were analyzed offline using conventional liquid nebulization ICP-OES or ICP-MS. This approach has two distinctive advantages: first it avoids a laborious sample digestion, which might be challenging for some technologically advanced materials, second it enables the use of ready to hand liquid standards, as the nanoparticles are completely ionized in the ICP if they are small enough [39]. To extend the capabilities of this method, recently LASIL was realized in an online approach, [40] which evades all manually performed sample handling steps. Moreover, online analysis of the generated nanoparticle suspension enables spatially resolved investigations, i.e., imaging [41] and depth profiling. Initial experiments performed in the work of Bonta et al. [40] for a material similar to the one used in this study indicated an ablation rate in the order of 35 nm per shot for strontium titanate (STO), which is a considerable improvement when compared to the depth profiling capabilities of conventional LA-ICP-MS with nanosecond laser instrumentation [27,28].

In this work, the applicability of online-LASIL for assessment of the platinum decoration on the surface of LSF electrodes has been investigated. After careful optimization, the procedure enabled the selective analysis of the surface decoration with platinum, moreover, the homogeneity of the platinum distribution could be monitored by spatially resolved measurements of the samples.

Table 1
Instrument operating conditions.

Laser NWR 213		ICP-MS	
Laser Fluence	1.2 J/cm^2	RF Power	1400 W
Spot Size	50 μm	Nebulizer gas flow rate (Ar)	1 L/min
Scanning Speed	50 μm/s	Cool gas flow rate (Ar)	14 L/min
Repetition Frequency	2 Hz	Auxiliary gas flow rate (Ar)	0.65 L/min
Ablated Area	0.35 mm^2	Dwell Time	0.05 s
Liquid carrier solution flow	0.5 mL/min	Monitored isotopes	^{194}Pt, ^{196}Pt, ^{115}In, ^{139}La, ^{90}Zr

2. Experimental

2.1. Reagents

Ultrapure water was prepared with a Barnstead EASYPURE II water system (ThermoFisher Scientific, USA), single element ICP standards were purchased from Merck (Germany), as well as hydrochloric acid (HCl) and nitric acid (HNO_3) and all chemicals not otherwise mentioned at least of analytical grade.

2.2. Instrumentation

For laser ablation, a NWR213 laser ablation system (ESI, USA), operating at a wavelength of 213 nm, was used. A quadrupole ICP-MS iCAP Qc (ThermoFisher Scientific, Germany) instrument with the standard cyclonic spray chamber and PFA nebulizer was used for analyte detection, as well as for liquid reference analysis and operated without collision gas, the applied instrumental settings are listed in Table 1. For the liquid reference analysis, in this case instead of the LASIL cell, an autosampler (SC-2-DX, ESI, USA) combined with an ESI Fast valve (ESI, USA) were connected with the sample introduction system. Data were collected using the instrument software, Qtegra Version 2.8. For imaging experiments, the raw platinum ICP-MS signal was background corrected using OriginPro 2020 (OriginLab Corporation, USA), images were created then with ImageLab Software (version 2.99, Epina GmbH, Austria), normalizing the platinum signal to the indium internal standard for correction of instrumental drift during the data acquisition. One way ANOVA (analysis of variance) was performed in Excel (Microsoft Cooperation, USA), to access the homogeneity of images. Measurement of crater depths was performed using a Dektak XT (Bruker, USA) stylus profilometer. The size distribution of the nanoparticles generated in the LASIL process was determined by particle tracking (ZetaView, Particle Metrix, Germany).

2.3. LASIL setup and measurements

The LASIL setup used in this work is mostly similar to that one described in [42]. In short, the sample is placed in a cavity of the PEEK body, which allows to flush the surface of the investigated 5x5x0.5 mm samples with the carrier solution. The fluid path over the sample is determined by the 2 mm wide channel in the polydimethylsiloxane (PDMS) spacer (thickness 500 μm), which also seals the cell. See Supplementary Fig. 1 and [42] for a more detailed information. On top a UV-transparent fused silica window is placed. The carrier fluid is

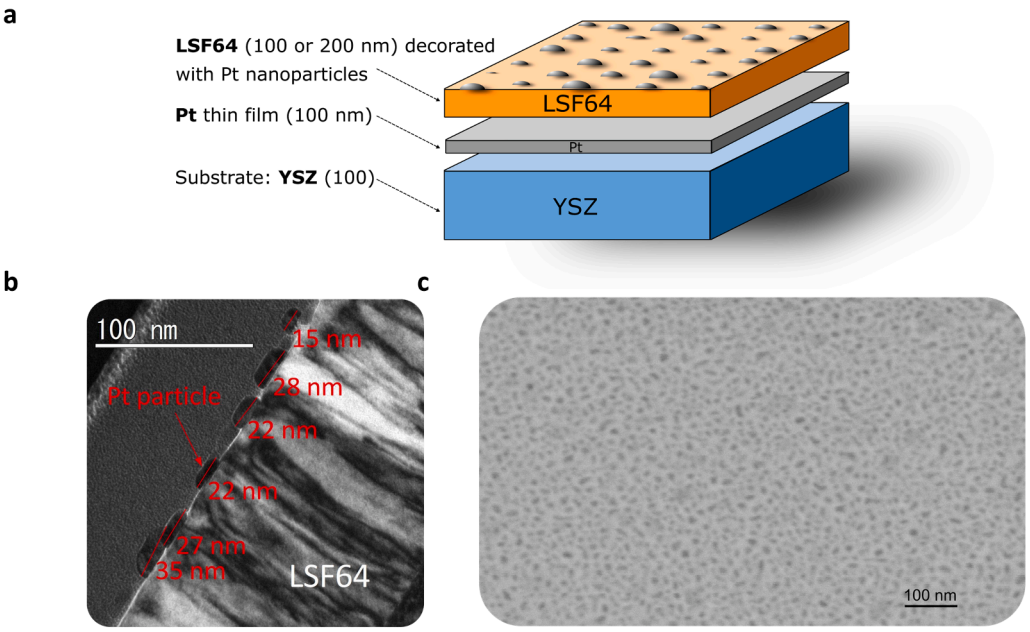

Fig 1. a: Schematic of the samples consisting of a YSZ substrate, a platinum current collector electrode, a LSF thin film and platinum nanoparticles as surface decoration, b: TEM image of cross section showing the platinum nanoparticles on the surface, c: A high resolution SEM image of the surface decoration, showing individual platinum nanoparticles with a size of about 20 nm [21].

pumped by a peristaltic pump (Perimax 12, SPETEC, Germany). All tubing was made of PFA, with an inner diameter of 0.5 mm on the input side to the cell and 0.25 mm between the cell and the ICP-MS instrument, to ensure a fast washout and transport of the analyte particles. The LASIL cell is placed in the ablation chamber of the NWR213 laser. To correct for eventual drifts during the measurement indium as internal standard with a concentration of 1 ng/g was added to all carrier solutions.

Prior to measurement the ICP-MS instrument was tuned for a maximum ^{115}In signal. For sample analysis on each sample 3 patterns using the laser parameters listed in Table 1 were measured. Transient signals were collected and integrated with the Qtegra software and normalized to the signal observed for ^{115}In used as internal standard.

2.4. Production of samples

Dense $La_{0.6}Sr_{0.4}FeO_{3-\delta}$ (LSF) thin films were prepared on one-side polished yttria stabilized zirconia single crystals (1 0 0) (YSZ) (Crystec, Germany). LSF powder was synthesized via the Pechini route [43] from Fe, La_2O_3 and $SrCO_3$ and the pulsed laser deposition (PLD) target was then prepared by isostatic pressing (150 MPa) and sintering at 1200 °C for 12 h. Laser deposition was performed at 600 °C substrate temperature (measured with a pyrometer) and 0.04 mbar oxygen partial pressure (Alphagaz, 99.995%) with a KrF excimer laser (Lambda COMPexPro 201F, wavelength 248 nm) at a frequency of 5 Hz, a laser energy of 2 J/cm^2 and a target to substrate distance of 6 cm. The deposition time was 30 min (9000 pulses) leading to a LSF thickness of 100 nm. LSF thin films were then decorated with platinum via magnetron sputter deposition (Baltech MED-020, Liechtenstein) for 2 s at an argon pressure of 2*10^{-2} mbar and a sputter current of 100 mA. However, to vary the deposited platinum amount, the sputter current (between 20 mA and 100 mA) and the sputter duration (between 2 and 5 s) were also varied. A cross section of the sample as well as electron microscopic image of the platinum decoration are shown in Fig. 1 The thickness of the LSF thin film was determined by introducing holes in the thin film by applying YSZ paste before the PLD step, which was removed afterwards by rinsing with ethanol. The film thickness was then determined by stylometric measurements with a Dektak XT (Bruker, USA).

2.5. Reference sample analysis

For verification of the online-LASIL measurements, samples without platinum current collector were produced. Those samples were digested with 1 mL aqua regia (3:1 HCl: HNO_3) in 15 mL polypropylene tubes in a water bath at 60 °C for 10 min. The samples were then diluted with ultrapure water to a final mass of 10 g. From this solution three aliquots per sample were further diluted 1:100 with 1% (v/v) HNO_3, and after addition of indium to obtain a concentration of 1 ng/g of this element in the samples, they were analyzed by solution nebulization (NEB) ICP-MS. Calibration solutions (ranging from 0.1 to 10 ng/g prepared in 1% (v/v) HNO_3 were used for calibration.

3. Results and discussion

3.1. Optimization of the carrier solution

Although the production of nanoparticles via laser ablation in liquid is an industrial process, careful optimization of the applied fabrication parameters is necessary to achieve nanoparticle with the desired dimensions. Indeed, particle characteristics such as size, shape and colloidal stability can vary over a wide range and depends on the properties of the used liquid medium. For online LASIL analysis the nanoparticles size must be small enough to prevent deposition in the system, enabling an efficient transport of the particles from the LASIL cell to the ICP-MS. Moreover, smaller particles are also beneficial for the measurement step, since atomization and ionization of larger particles can be incomplete. On top of that, preliminary experiments showed that only a part of the ablated material is transferred into suspended nanoparticles, another part becomes dissolved in the carrier solution. These analyte ions need to be stabilized to prevent unwanted losses due to adsorption of analyte on the walls of the LASIL cell, the applied transport tubing, the nebulizer, or the spray chamber of the sample introduction system.

In more conventional analysis, solutions are usually acidified to prevent analyte loss due to adsorption, or organic additives are used to complex the analyte ion [44]. As LSF would dissolve in concentrated acid [15] and the carrier solutions needs to be transparent in the

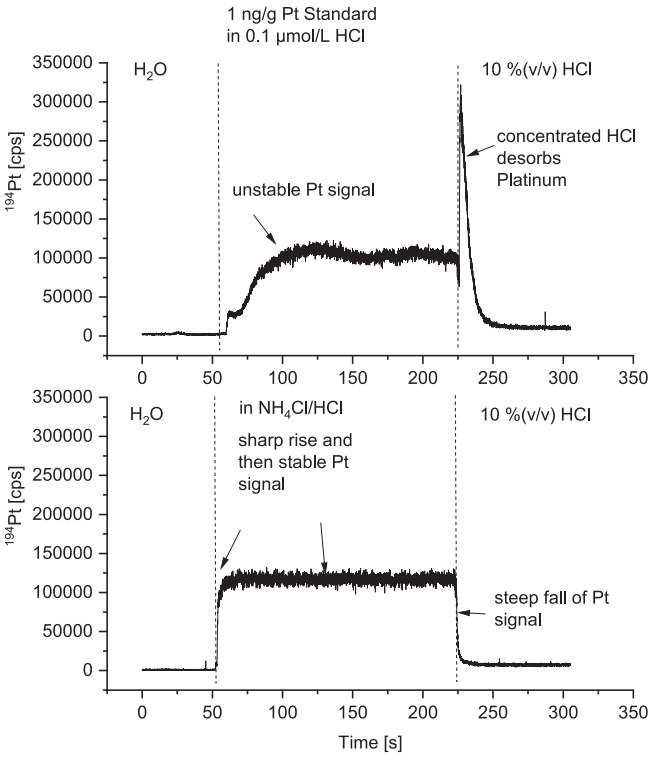

Fig 2. Optimization of carrier solution composition: To optimize the solvent conditions a 1 ng/g platinum standard solution was injected into the LASIL setup. After the signal has stabilized an acid solution (10% (v/v)) HCl was injected to desorb all platinum from the tubing walls. Top: Using only very diluted (1 µmol/L) HCl yields to adsorption of platinum, which gives a slow response in the signal and a large peak of the adsorbed platinum after switching to concentrated HCl. Bottom: Using the optimized NH_4Cl/HCl solution concentration the platinum signal drops fast to the baseline after the switching to concentrated HCl, indicating that no adsorption has occurred. Further the rise of the signal is much faster, and the achieved plateau is much more stable than with diluted acid alone.

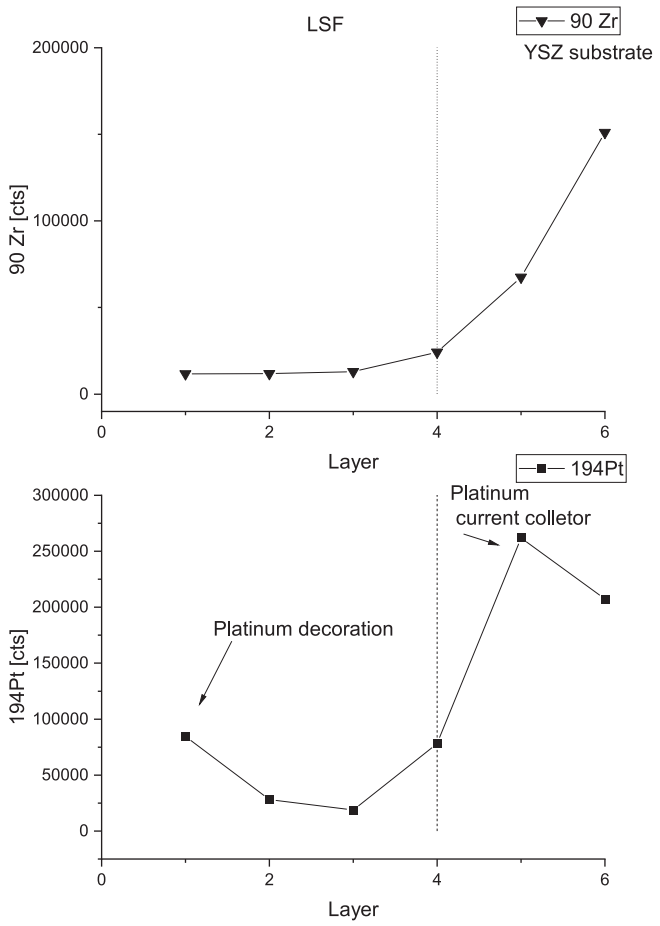

Fig 3. Depth profile of ^{90}Zr (top) and ^{194}Pt (bottom) for sample with a platinum decorated 200 nm thick LSF thin film and a platinum current collector beneath. The depth of one ablation layer is approximately 60 nm. The platinum decoration on top of the LSF can clearly be separated from the platinum current collector beneath, as the platinum signal is high in the first layer, stemming from the surface decoration, then drops, and rises again in the 4th ablation layer, as the platinum current collector is reached. In the 5th ablation layer, the rising zirconium signal indicates that the YSZ substrate has been ablated.

ultraviolet region at 213 nm, which rules out many organic compounds, this approach could not be used in the current application. Thus, different combinations of diluted hydrochloric acid and ammonia chloride were investigated. These substances are transparent in the ultraviolet light range and the excess of chloride ions can form stronger complexes with platinum ions to stabilize them. The investigated NH_4Cl/HCl mixing solutions resulted in weak acidic conditions, which did not harm the integrity of the LSF thin film while preventing losses of the ions formed in the LASIL process due to adsorption or precipitation of cations.

Fig. 2 summarizes the optimization of the carrier solution. First, water is pumped through the LASIL cell with a plain YSZ single crystal replacing the actual sample, then the carrier solution is switched to a 1 ng/g platinum standard in the medium of interest – 30 mmol/L HCl in the shown experiment. As can be deduced from Fig. 2 there was no sudden increase in the platinum signal, instead a continuous rise over a period of roughly 50 s was observed until the ICP-MS platinum signal has stabilized. Then, the carrier is switched to a 10% (v/v) HCl, resulting in a sharp increase of the platinum-signal, which decreased quickly to background level. This outcome indicates that a part of platinum in the introduced standard was lost during transport from the LASIL cell to the ICP-MS, since diluted HCl could not prevent the retention of platinum on the surface of LASIL cell or applied transport tubing. Purging of the system with concentrated HCl results in a release of the platinum species which have been adsorbed in the system.

A completely different behavior was observed when using the optimized carrier solution containing NH_4Cl and HCl. Switching from water as carrier solution to the NH_4Cl/HCl-solution containing 1 ng/g platinum results in an abrupt rise of the signal, reaching constant level without any further decrease. When switching from this platinum standard to 10% (v/v) HCl as purge solution, no desorption of platinum was observed, but a fast drop of the signal to baseline level occurred. This result indicates that no adsorption and thus no analyte loss has occurred with the use of platinum in NH_4Cl/HCl medium (Fig. 2). The optimized condition was found to be 30 mmol/L hydrochloric acid and 910 mmol/L NH_4Cl, with pH of 5, giving the best stabilization of the platinum ions, while not attacking the LSF.

3.2. Optimization of depth resolution

3.2.1. Single spot measurements

For differentiation of the platinum decoration from the current collector a sufficient depth resolution is required. Therefore, the parameters for sample ablation and transport of the generated nanosol to the detection device have to be carefully optimized, in particular the effect of the carrier solution flow rate and the laser energy. The ablation rate at these optimized conditions (Table 1) was determined by measuring a series of single spots with a profilometer (Dektak XT), which yielded an average ablation of 30 nm per shot. This is in good agreement to previous work [40], where 35 nm per shot were found for strontium

titanate (STO), a similar ceramic material. However, the platinum signals observed for individual spots varied leading to a difficult data interpretation. This can be to one part attributed to the limited signal intensity due to the low coverage of the surface, which therefore yields a poor signal to noise ratio. To the other part, it is not clear if the decoration provides sufficient homogeneity. Therefore, an improved approach is required for the quantitative determination of the platinum decoration.

3.2.2. Measurement of line patterns

To circumvent possible problems with sample inhomogeneity and to give a higher signal for an improved signal to noise ratio, a larger area was ablated with line scans. Repetition rate and scan speed were chosen to allow an overlap between the individual laser spots, resulting in the application of 2 laser spots per position (Table 1). Considering the ablation rate per laser shot of approximately 30 nm this procedure should still provide sufficient depth resolution for differentiation between surface decoration and collector grid. That only the uppermost layer of platinum was ablated was confirmed by measuring two samples with 100 nm thick LSF thin film from the same decoration process, i.e., the same amount of platinum on the top, where one sample was fabricated with and one sample without a current collector. These two samples gave the same platinum signal for the surface decoration ($p = 0.96$). Completeness of platinum removal was controlled by a second measurement of the investigated sample locations using identical LASIL conditions. As expected, the analysis of the sample with no current collector platinum showed signals comparable to the experimental blank, whereas for the samples with current collector a significant increase in the platinum signal was observed.

Using optimized laser conditions, a depth profile was recorded by passing the pattern six times over a sample with a 200 nm thick LSF film (Fig. 3). The platinum signal from the surface decoration is the highest signal in the first ablation layer and drops remarkably in the second and third ablation layer. The fourth ablation layer shows a significant increase in the Pt-signal, indicating that with this ablation layer the current collector has been reached. Contrary results were found for Zr, which is a constituent of the substrate. Signals close to the background level were observed for the first three layers, a slight increase was observed for layer four, and strongly rising signals for the layers five and six. This signal sequence indicates that the first three layers were made only of LSF, the fourth layer partially hit the YSZ substrate, and layers 5 and 6 belong definitively to the YSZ substrate. This outcome is consistent with the findings derived for the ablation rate. As mentioned before the applied LASIL parameters enabled the removal of approximately 30 nm material per laser shot. Thus, with three ablation layers six shots were fired per sample location, resulting in the ablation of around 180 nm deep– up to this sample depth only signals from the surface decoration and the LSF could be expected. With the fourth layer a sample depth of ~240 nm has been reached, hence, there should be signals from the current collector and the YSZ substrate.

For comparison, the same sample was ablated using a conventional 213 nm laser system and single shot ablation mode. Helium was used as carrier gas with a flow of 650 mL/min, argon makeup gas with a flow of 0.8 L/min was added using a concentric mixer.

It was not possible to separate the two layers of platinum, the platinum signal showed a huge intensity for the very first shot, and then decreases approximately to one tenth of the signal with the second shot, whereas the third and all further laser shots revealed signals close to background level. The presence of a high zirconium signal from the YSZ substrate in the first shot, which increased slightly with the second shot and remained constant afterwards, indicated that even with this first shot the substrate has been reached. This result clearly points to a simultaneous ablation of Pt-decoration, LSF thin film and platinum current collector with the employed ns LA-system. Profilometric measurements of the obtained ablation crater revealed an ablation rate of 200 nm per shot, which is clearly not sufficient for the current application.

3.3. Measurements of platinum decoration

From conventional laser ablation ICP-MS it is known that the ablated material is not quantitatively transported to the plasma, due to redeposition of particles. Transport efficiency was about 40% in early studies, with highly optimized cell design and femtosecond lasers up to 80–90% can be achieved. [39,45,46]. In previously reported online-LASIL applications, only elemental ratios were of interest [40–42], where a potential loss of particles is not a problem as long as elemental fractionation is corrected [47]. Even though preliminary experiments with a particle tracking analyzer revealed that the size distribution of the particles produced in LASIL experiments ranges from 20 to 200 nm, the quantitative transport of these particles from the LASIL cell to the ICP-MS is unlikely. This assumption is confirmed by single particle ICP-MS measurements [48], which correct losses of nanoparticles using reference materials for calibration, otherwise a time-consuming determination of transport efficiency and nebulization efficiency is necessary to yield reliable results. Thus, in the current study an absolute quantification of the platinum was not possible and so matrix matched standards have to be used to compensate transport losses of the generated nanosol.

Since for the investigated material no reference material is available, an in-house reference was produced via PLD and sputter coating. For this purpose, four samples with identical platinum surface coverage on LSF thin films were fabricated, three without and one with platinum current collector beneath. The sample with current collector served as one-point calibration standard for quantitative LASIL measurements, the other three samples were used for chemical analysis of the surface decoration using NEB ICP-MS. Therefore, the three samples without current collector were digested and the platinum content determined using NEB ICP-MS. See section 2.5 for details. The mean surface coverage of these samples was 33.3 ± 1.7 ng/mm^2 ($n = 3$).

To check for a complete digestion of platinum surface decoration the substrates were subjected to a second digestion using identical conditions. ICP-MS analysis of the derived sample solutions gave signals comparable to procedural blank solutions, demonstrating that the platinum decoration has been quantitatively dissolved in the first digestion step.

To test the capabilities of the LASIL method a series of four samples was produced with platinum decorations varying over a wider range. For each platinum concentration level, a set of two identical samples was produced, one with current collector for the LASIL measurements and one without current collector, which has been used for validation of the determined surface decoration. This reference sample without current collector was subjected to digestion and platinum determination using NEB ICP-MS.

The samples with platinum current collector were measured by LASIL and quantified using matrix matched standard for calibration as described above. On each sample three patterns were measured, the RSD (relative standard deviation) of the derived results was about 5%, which is consistent with the RSD values using digestion of the samples in combination with subsequent analyte determination by NEB ICP-MS. The limit of detection (LOD) of the LASIL method is 0.02 ng/mm^2 platinum, determined as described in [49], which is more than sufficient for the application of materials like those investigated in this work. The platinum surface coverage varied in the range from 30 to 106 ng/mm^2 platinum, the surface coverage showing the best electrochemical performance is 46 ng/mm^2.

The surface coverage obtained with online-LASIL showed a highly linear correlation ($R^2 = 0.99$) with the reference values obtained by NEB ICP-MS. The root mean square error of prediction (RMSE) for the samples was 5.3 ng/mm^2 platinum, a maximum deviation of 18% between LASIL results and those obtained using NEB ICP-MS was found for the sample with a Pt-decoration of 30 ng/mm^2, the minimum deviation was found to be 4% for a Pt-decoration with 106 ng/mm^2.

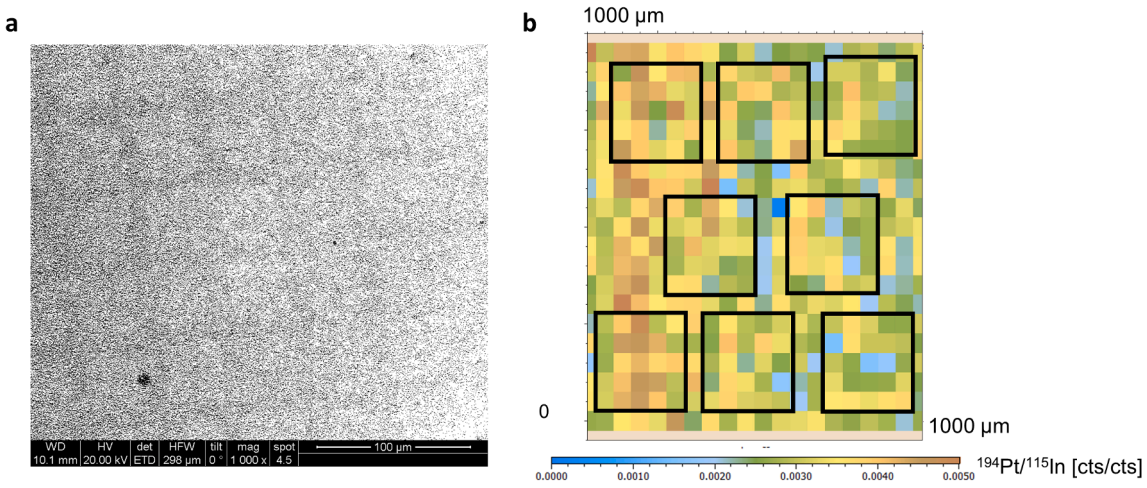

Fig 4. a: SEM image providing information about the homogeneity of the platinum surface coverage, note that the slight grid is an artifact caused from the reuse of YSZ substrates, which have been passed through an ion etching processes prior to the application in this work. For a better contrast, the image is binarized using ImageJ (version 1.52b), b: Mapping of the ^{194}Pt surface signal normalized to ^{115}In over a representative part of a sample, the black frames indicate the sample areas used for ANOVA analysis.

3.4. Homogeneity assessment

In previous work, the electrochemical characterization was performed with macroscopic samples, so only relationships between the mean surface coverage of the whole sample and the electrochemical performance were accessible. However, in future investigations measurements might be scaled down using different methods of sample preparation, thus better information about the uniformity of the distribution of the platinum nanoparticles is of interest. From SEM images (Fig. 4a and Fig. 1c) such distribution cannot be assessed with confidence, if the Pt-decoration of the sample is homogeneous or if there is a gradient present. As online LASIL allows to record spatially resolved, quantitative elemental data [41], it is the ideal method for this task.

To test the uniformity of the platinum decoration, a sample area of 1x1 mm^2 was imaged using the parameters presented in Table 1. Measurement carried out to generate the platinum distribution image (Fig. 4b) with a resolution of 20x20 pixel took 2 h. In the imaged sample area, there are some areas with higher, and others with lower Pt-coverage. The RSD of all pixel intensities is 25%, which can be regarded as the microscopic inhomogeneity due to the stochastic variations resulting from the low surface coverage. To access the overall homogeneity a one-way ANOVA (analysis of variance) was performed. Within the imaged sample area eight 5x5 groups of pixels were chosen (for details see Fig. 4b) and the variability within and between them was evaluated. The ANOVA revealed that there was a significant variation ($F = 6.88$, $p = 2.6*10^{-7}$) of the surface coverage within the investigated area. Having this information in mind is important for future investigations, as with different production processes a higher level of uniformity of the platinum coverage can be achieved, which can be accessed with this method.

4. Conclusion

In this work, we exploited the capabilities of online LASIL for the absolute quantification of the platinum surface decoration of LSF thin films, a promising material for SOFC electrodes. In contrast to previously reported applications focused on the determination of the overall thin film stoichiometry demands this task investigations with sufficient surface sensitivity. Moreover, instead of bulk components the analysis of trace constituents is mandatory. To fulfill these requirements a thorough optimization of the ablation parameters was necessary, resulting in an improved depth resolution for online LASIL when compared to conventional LA-ICP-MS. The ablation per shot for LSF was found to be in the order of 30 nm deep with online-LASIL, compared to approximately 200 nm for LA-ICP-MS. This improved depth resolution was beneficial for the analysis of the surface decoration of platinum on LSF electrodes. It was possible to separate the platinum decoration on top of the electrodes, from the platinum current collector, which lies buried in the depth of 100 nm. However, performed experiments indicated that LASIL generates not only nanoparticles, a fraction of the ablated sample material also becomes dissolved. Thus, a careful optimization of the carrier solution is necessary to avoid losses of the dissolved part of the ablated material, while not harming the integrity of the LSF electrode. Platinum signal could be quantified using a matrix matched standard for calibration. The platinum amount per area determined in the surface coverages showed a good agreement with liquid reference values determined for samples prepared without current collector electrode. A main advantage of online LASIL is the possibility of analyzing spatially resolved element distributions. A sample area of 1x1 mm^2 was imaged with a resolution of 50 µm. This revealed that the samples show some degree of inhomogeneity on the microscopic level, which is an important information for further optimization of the LSF production process.

Funding

This work was supported by the Austrian Science Fund-FWF grant P31165-N37.

CRediT authorship contribution statement

Maximilian Weiss: Investigation, Writing - original draft. **Christoph Riedl:** Investigation, Writing - review & editing. **Johannes Frank:** Investigation, Resources. **Jürgen Fleig:** Supervision, Resources, Writing - review & editing. **Andreas Limbeck:** Supervision, Conceptualization, Project administration, Resources, Writing - review & editing.

Declaration of Competing Interest

The authors declare that they have no known competing financial interests or personal relationships that could have appeared to influence the work reported in this paper.

Acknowledgements

We want to thank Elisabeth Eitenberger for conduction of SEM images and the University Service Centre for Transmission Electron

Microscopy of the TU Wien (USTEM) for providing SEM and TEM measurements.

Appendix A. Supplementary data

Supplementary data to this article can be found online at https://doi.org/10.1016/j.microc.2021.106236.

References

[1] E. Ivers-Tiffée, A. Weber, D. Herbstritt, Materials and technologies for SOFC-components, J. Eur. Ceram. Soc. 21 (2001) 1805–1811.
[2] K.M. El-Khatib, R.M. Abdel Hameed, R.S. Amin, A.E. Fetohi, Core-shell structured Pt-transition metals nanoparticles supported on activated carbon for direct methanol fuel cells, Microchem. J. 145 (2019) 566–577.
[3] E.D. Wachsman, K.T. Lee, Lowering the temperature of solid oxide fuel cells, Science 334 (2011) 935–939.
[4] B.A. Boukamp, Fuel cells: the amazing perovskite anode, Nat. Mater. 2 (5) (2003) 294–296.
[5] A. Nenning, L. Volgger, E. Miller, L.V. Mogni, S. Barnett, J. Fleig, The electrochemical properties of Sr(Ti, Fe)O3-δ for anodes in solid oxide fuel cells, J. Electrochem. Soc. 164 (4) (2017) F364–F371.
[6] W. Jung, H.L. Tuller, Impedance study of SrTi1−xFexO3−δ (x=0.05 to 0.80) mixed ionic-electronic conducting model cathode, Solid State Ionics 180 (11-13) (2009) 843–847.
[7] S.-L. Zhang, D. Cox, H. Yang, B.-K. Park, C.-X. Li, C.-J. Li, S.A. Barnett, High stability SrTi1−xFexO3−δ electrodes for oxygen reduction and oxygen evolution reactions, J. Mater. Chem. A 7 (37) (2019) 21447–21458.
[8] E. Navickas, T.M. Huber, Y. Chen, W. Hetaba, G. Holzlechner, G. Rupp, M. Stöger-Pollach, G. Friedbacher, H. Hutter, B. Yildiz, J. Fleig, Fast oxygen exchange and diffusion kinetics of grain boundaries in Sr-doped LaMnO3 thin films, Phys Chem Chem Phys 17 (12) (2015) 7659–7669.
[9] S. Kogler, A. Nenning, G.M. Rupp, A.K. Opitz, J. Fleig, Comparison of electrochemical properties of La0.6Sr0.4FeO3-δthin film electrodes: oxidizing vs. reducing conditions, J. Electrochem. Soc. 162 (3) (2015) F317–F326.
[10] A. Schmid, G.M. Rupp, J. Fleig, Voltage and partial pressure dependent defect chemistry in (La, Sr)FeO3-delta thin films investigated by chemical capacitance measurements, Phys. Chem. Chem. Phys. 20 (2018) 12016–12026.
[11] R. Küngas, A.S. Yu, J. Levine, J.M. Vohs, R.J. Gorte, An investigation of oxygen reduction kinetics in LSF electrodes, J. Electrochem. Soc. 160 (2) (2013) F205–F211.
[12] M. Kuhn, S. Hashimoto, K. Sato, K. Yashiro, J. Mizusaki, Oxygen nonstoichiometry, thermo-chemical stability and lattice expansion of La0.6Sr0.4FeO3−δ, Solid State Ionics 195 (1) (2011) 7–15.
[13] J. Januschewsky, M. Ahrens, A. Opitz, F. Kubel, J. Fleig, Optimized La0.6Sr0.4CoO3-δ thin-film electrodes with extremely fast oxygen-reduction kinetics, Adv. Funct. Mater. 19 (19) (2009) 3151–3156.
[14] M. Kubicek, A. Limbeck, T. Frömling, H. Hutter, J.r. Fleig, Relationship between cation segregation and the electrochemical oxygen reduction kinetics of La0.6Sr0.4CoO3−δ thin film electrodes, J. Electrochem. Soc. 158 (6) (2011) B727, https://doi.org/10.1149/1.3581114.
[15] G.M. Rupp, H. Téllez, J. Druce, A. Limbeck, T. Ishihara, J. Kilner, J. Fleig, Surface chemistry of La0.6Sr0.4CoO3−δ thin films and its impact on the oxygen surface exchange resistance, J. Mater. Chem. A 3 (45) (2015) 22759–22769.
[16] N. Tsvetkov, Q. Lu, L. Sun, E.J. Crumlin, B. Yildiz, Improved chemical and electrochemical stability of perovskite oxides with less reducible cations at the surface, Nat Mater 15 (2016) 1010–1016.
[17] H.J. Hwang, J.-W. Moon, S. Lee, E.A. Lee, Electrochemical performance of LSCF-based composite cathodes for intermediate temperature SOFCs, J. Power Sources 145 (2005) 243–248.
[18] F. Baumann, J. Fleig, H. Habermeier, J. Maier, Impedance spectroscopic study on well-defined (La, Sr)(Co, Fe)O3−δ model electrodes, Solid State Ionics 177 (2006) 1071–1081.
[19] F. Baumann, J. Fleig, H. Habermeier, J. Maier, Ba0.5Sr0.5Co0.8Fe0.2O3−δ thin film microelectrodes investigated by impedance spectroscopy, Solid State Ionics 177 (2006) 3187–3191.
[20] M. Burriel, C. Niedrig, W. Menesklou, S.F. Wagner, J. Santiso, E. Ivers-Tiffée, BSCF epitaxial thin films: electrical transport and oxygen surface exchange, Solid State Ionics 181 (13-14) (2010) 602–608.
[21] C. Riedl, A. Schmid, A. Nenning, H. Summerer, S. Smetaczek, S. Schwarz, J. Bernardi, A. Optiz, A. Limbeck, J. Fleig, Outstanding oxygen reduction kinetics of La0.6Sr0.4FeO3−δ surfaces decorated with platinum nanoparticles, J. Electrochem. Soc. 167 (2020) 104514, https://doi.org/10.1149/1945-7111/ab9c7f.
[22] A. Limbeck, M. Bonta, W. Nischkauer, Improvements in the direct analysis of advanced materials using ICP-based measurement techniques, J. Anal. At. Spectrom. 32 (2017) 212–232.
[23] S. Turková, M. Vašinová Galiová, K. Štůlová, Z. Čadková, J. Száková, V. Otruba, V. Kanický, Study of metal accumulation in tapeworm section using laser ablation-inductively coupled plasma-mass spectrometry (LA-ICP-MS), Microchem. J. 133 (2017) 380–390.
[24] A. Hanć, A. Małecka, A. Kutrowska, A. Bagniewska-Zadworna, B. Tomaszewska, D. Barałkiewicz, Direct analysis of elemental biodistribution in pea seedlings by LA-ICP-MS, EDX and confocal microscopy: Imaging and quantification, Microchem. J. 128 (2016) 305–311.
[25] J. Pisonero, B. Fernández, D. Günther, Critical revision of GD-MS, LA-ICP-MS and SIMS as inorganic mass spectrometric techniques for direct solid analysis, J. Anal. At. Spectrom. 24 (9) (2009) 1145, https://doi.org/10.1039/b904698d.
[26] G. Friedbacher, H. Bubert, Surface and Thin Film Analysis, Weinheim, Germany, 2011.
[27] J. Pisonero, D. Gunther, Femtosecond laser ablation inductively coupled plasma mass spectrometry: fundamentals and capabilities for depth profiling analysis, Mass Spectrom Rev 27 (2008) 609–623.
[28] D. Käser, L. Hendriks, J. Koch, D. Günther, Depth profile analyses with sub 100-nm depth resolution of a metal thin film by femtosecond – laser ablation – inductively coupled plasma – time-of-flight mass spectrometry, Spectrochim. Acta, Part B 149 (2018) 176–183.
[29] A. Limbeck, P. Galler, M. Bonta, G. Bauer, W. Nischkauer, F. Vanhaecke, Recent advances in quantitative LA-ICP-MS analysis: challenges and solutions in the life sciences and environmental chemistry, Anal. Bioanal. Chem 407 (2015) 6593–6617.
[30] Y. Ke, Y. Sun, P. Lin, J. Zhou, Z. Xu, C. Cao, Y. Yang, S. Hu, Quantitative determination of rare earth elements in scheelite via LA-ICP-MS using REE-doped tungstate single crystals as calibration standards, Microchem. J. 145 (2019) 642–647.
[31] A. Hanć, A. Olszewska, D. Barałkiewicz, Quantitative analysis of elements migration in human teeth with and without filling using LA-ICP-MS, Microchem. J. 110 (2013) 61–69.
[32] A. Hanć, P. Zduniak, K. Erciyas-Yavuz, A. Sajnóg, D. Barałkiewicz, Laser ablation-ICP-MS in search of element pattern in feathers, Microchem. J. 134 (2017) 1–8.
[33] H. Zeng, X.-W. Du, S.C. Singh, S.A. Kulinich, S. Yang, J. He, W. Cai, Nanomaterials via laser ablation/irradiation in liquid: a review, Adv. Funct. Mater. 22 (7) (2012) 1333–1353.
[34] G. Yang, Laser ablation in liquids: applications in the synthesis of nanocrystals, Prog. Mater Sci. 52 (2007) 648–698.
[35] E.V. Muravitskaya, V.A. Rosantsev, M.V. Belkov, E.A. Ershov-Pavlov, E. V. Klyachkovskaya, Laser ablation in liquids as a new technique of sampling in elemental analysis of solid materials, Spectrochim. Acta, Part B 64 (2) (2009) 119–125.
[36] D.N. Douglas, J.L. Crisp, H.J. Reid, B.L. Sharp, Laser ablation of a sample in liquid—LASIL, J. Anal. At. Spectrom. 26 (6) (2011) 1294, https://doi.org/10.1039/c0ja00144a.
[37] S. Okabayashi, T.D. Yokoyama, Y. Kon, S. Yamamoto, T. Yokoyama, T. Hirata, Evaluation of Laser Ablation in Liquid (LAL) technique as a new sampling technique for elemental and isotopic analysis using ICP-mass spectrometry, J. Anal. At. Spectrom. 26 (7) (2011) 1393, https://doi.org/10.1039/c0ja00200c.
[38] R. Machida, T. Nakazawa, Y. Sakuraba, M. Fujiwara, N. Furuta, Particle size-related elemental fractionation in laser ablation in liquid inductively coupled plasma mass spectrometry, J. Anal. At. Spectrom. 30 (2015) 2412–2419.
[39] L. Ebdon, M.E. Foulkes, S. Hill, Direct atomic spectrometric analysis by slurry atomisation. Part 9. Fundamental studies of refractory samples, J. Anal. At. Spectrom. 5 (1) (1990) 67, https://doi.org/10.1039/ja9900500067.
[40] M. Bonta, J. Frank, S. Taibl, J. Fleig, A. Limbeck, Online-LASIL: Laser Ablation of Solid Samples in Liquid with online-coupled ICP-OES detection for direct determination of the stoichiometry of complex metal oxide thin layers, Anal Chim Acta 1000 (2018) 93–99.
[41] C. Herzig, J. Frank, A.K. Opitz, J. Fleig, A. Limbeck, Quantitative imaging of structured complex metal oxide thin films using online-LASIL-ICP-MS, Talanta 217 (2020) 121012, https://doi.org/10.1016/j.talanta.2020.121012.
[42] C. Herzig, J. Frank, A.K. Opitz, J. Fleig, A. Limbeck, Quantitative analysis of gadolinium doped cerium oxide thin films via online-LASIL-ICP-OES, J. Anal. At. Spectrom. 34 (11) (2019) 2333–2339.
[43] M.P. Pechini, Method of Preparing Lead and Alkaline Earth itanates and Niobates and Coating Method Using the Same to Form a Capacitor, US Patent US3330697A, Sprague Electric Co., US Patent US3330697A, 1967.
[44] E. Ivanova, F. Adams, Flow injection on-line sorption preconcentration of platinum in a knotted reactor coupled with electrothermal atomic absorption spectrometry, Fresen. J. Anal. Chem. 361 (1998) 445–450.
[45] C.C. Garcia, H. Lindner, K. Niemax, Transport efficiency in femtosecond laser ablation inductively coupled plasma mass spectrometry applying ablation cells with short and long washout times, Spectrochim. Acta, Part B 62 (1) (2007) 13–19.
[46] S.J.M. Van Malderen, A.J. Managh, B.L. Sharp, F. Vanhaecke, Recent developments in the design of rapid response cells for laser ablation-inductively coupled plasma-mass spectrometry and their impact on bioimaging applications, J. Anal. At. Spectrom. 31 (2016) 423–439.
[47] S. Zhang, M. He, Z. Yin, E. Zhu, W. Hang, B. Huang, Elemental fractionation and matrix effects in laser sampling based spectrometry, J. Anal. At. Spectrom. 31 (2016) 358–382.
[48] M. Tharaud, P. Louvat, M.F. Benedetti, Detection of nanoparticles by single-particle ICP-MS with complete transport efficiency through direct nebulization at few-microlitres-per-minute uptake rates, Anal Bioanal Chem 413 (3) (2021) 923–933.
[49] J.-M. Mermet, Limit of quantitation in atomic spectrometry: An unambiguous concept? Spectrochim. Acta, Part B 63 (2) (2008) 166–182.